Original Article

Iranian Journal of Immunology

https://iji.sums.ac.ir

Identification of the Optimal Pattern of the Injection and Dosage of DC Immunotherapy Using the Mathematical Models Based on Ordinary Differential Equations

Bahareh Zand[1], Samaneh Arab[2,3], Nasim Kheshtchin[4,5], Abazar Arabameri[6], Mahboubeh Ashourpour[7], Davoud Asemani[8], Ehsan Sharif-Paghaleh[1,9], Farshid Nourbakhsh[1], Jamshid Hadjati[10*]

[1]Department of Immunology, School of Medicine, Tehran University of Medical Sciences, Tehran, Iran; [2]Nervous System Stem Cells Research Center, Semnan University of Medical Sciences, Semnan, Iran; [3]Department of Tissue Engineering and Applied Cell Sciences, School of Medicine, Semnan University of Medical Sciences, Semnan, Iran; [4]Department of Immunology, School of Medicine, Shiraz University of Medical Sciences, Shiraz, Iran; [5]Allergy Research Center, Shiraz University of Medical Sciences, Shiraz, Iran; [6]Department of Electrical Engineering, Faculty of Engineering, University of Zanjan, Zanjan, Iran; [7]Department of Pathobiology, School of Public Health, Tehran University of Medical Sciences, Tehran, Iran; [8]Laboratory of Signals and Electronic Systems, Faculty of electrical and computer Engineering, Khajeh Nasir Toosi University of Technology, Tehran, Iran; [9]Division of Imaging Sciences and Biomedical Engineering, St Thomas' Hospital, Faculty of Life Sciences and Medicine, King's College London, London, England; [10]Cancer Biology Research Center, Cancer Institute of Iran, Tehran University of Medical Sciences, Tehran, Iran

ABSTRACT

Background: Mathematical modeling offers the possibility to select the optimal dose of a drug or vaccine. Considerable evidence show that many bacterial components can activate dendritic cells (DCs). Our previous report showed that multiple doses of DCs matured with Listeria monocytogenes led to tumor regression whereas multiple doses of CpG-matured DCs affected tumor reversely.

Objective: To assess a combined pattern of DC vaccination proposed by a mathematical model for tumor regression.

Methods: WEHI164 cells were inoculated subcutaneously in the right flank of BALB/c mice. Bone marrow-derived DCs were matured by Listeria monocytogenes and CpG motifs. DCs were injected using specific patterns and doses predicted by mathematical modeling. Effector cell-mediated cytotoxicity, gene expression of T cell-related transcription factors, as well as tumor growth and survival rate, were assessed in different groups.

Results: Our study indicated that the proposed mathematical model could simulate the tumor and immune system interaction, and it was verified by decreasing tumor size in the List+CpG group. However, comparing the effect of different treatment modalities on Th1/Treg transcription factor expression or cytotoxic responses revealed no advantage for combined therapy over other treatment modalities.

Conclusions: These results suggest that finding new combinations of DC vaccines for the treatment of tumors will be promising in the future. The results of this study support the mathematical modelling for DC vaccine design. However, some parameters in this model must be modified to provide a more optimized therapy approach.

Keywords: Cancer vaccines, Dendritic cells, *Listeria monocytogenes*, CpG, Mathematical model

**Corresponding author:*
Jamshid Hadjati
Cancer Biology Research Center, Cancer Institute of Iran, Tehran University of Medical Sciences, Tehran, Iran
Email: hajatij@tums.ac.ir

Cite this article as:
Zand B, Arab S, Kheshtchin N, Arabameri A, Ashourpour M, Asemani D, Sharif-Paghaleh E, Nourbakhsh F, Hadjati J. Identification of the Optimal Pattern of the Injection and Dosage of DC Immunotherapy Using the Mathematical Models Based on Ordinary Differential Equations. *Iran J Immunol.* 2022; 19(1):1-17, doi: 10.22034/IJI.2022.91617.2092.

Received: 2021-06-16
Revised: 2021-11-03
Accepted: 2021-11-17

INTRODUCTION

Cancer is a major health problem that affects people all over the world, and it is the second leading cause of death following cardiovascular diseases in many countries (1-3). Conventional cancer therapies include surgery, chemotherapy, radiation therapy, hormone therapy, or a combination of these methods which also have side effects for patients. As a result, a great deal of research has recently been conducted to treat cancer by immunotherapy besides chemotherapy and radiation therapy (4, 5). Dendritic cell (DC)-based vaccination is a promising immunotherapy approach to induce antitumor immunity (6-8). DCs as major coordinators of the immune system are considered *professional antigen-presenting cells* (APCs) capable of activating naïve T cells (9).

Several studies have demonstrated protozoa, whole bacteria, and microbial components like lipopolysaccharide (LPS), CpG-DNA, and Poly I: C interacting with pattern recognition receptors (PRRs), such as toll-like receptors (TLR) on dendritic cells. This interaction can lead to increased expression of costimulatory molecules and also the DC maturation (10-13).

Mathematical models are useful tools for simulating and studying biological systems, providing researchers with new insights and opportunities to previse new cancer treatments and improve common therapies (14). The complex and non-linear action of tumors and the immune system have been the topic of many mathematical models up to now. In terms of the biological knowledge used to create these models, they can be divided into two categories including the black-box models and the white-box ones (15).

In the black-box models, such as artificial neural networks (ANNs), there is a lack of access to the internal workings or parameters of the model. The internal workings of these models are confusing and do not provide an estimate of the importance of each input variable to the model prediction. It is also difficult to comprehend how various inputs interact with one another. They rely solely on measured data from the actual system, without any theoretical presumption (16).

Although this technique is beneficial in systems where internal structures are unknown, this is not the case for systems such as tumor-immune system interactions, where much immunological knowledge has been gained from previous researches, and cannot make effective use of prior knowledge. As a result, this method has been used in only a few studies (such as (17) and (18)) in modeling tumor dynamics. To exemplify, a recursive neural network with a pharmacokinetic/pharmacodynamic model is presented to predict the optimal vaccination patterns in immunotherapy with dendritic cell vaccines. The ANN predicts an exponentially increasing pattern of the CpG-matured DC to be effective in suppressing tumor growth (17).

On the other hand, the white-box models are mainly constructed based on physiological knowledge of the system. One can explain how these models act, how they produce predictions, and what the influencing variables are (16). The ordinary differential equation (ODE), which is a white-box modeling approach, is the most prevalent tool in computational systems biology (19). It treats the biological system as a set of reaction-based equations and ensures that the reactions are continuous and deterministic. The equations in such models are usually nonlinear and can be analyzed theoretically and numerically based on their complexity.

Various ODE-based studies focus on modeling various aspects of tumor behavior, including tumor growth, angiogenesis (20), metastasis (21), tumor escape (22), dormancy (23), dynamical complexity (24), and optimization in Chemo/Immuno/Radiotherapy treatment (25-27). There are also several ODE models for immunotherapy based on the DCs, which mainly study the dynamics of the immune system during immunotherapy as well as the optimization of treatment patterns in vaccine therapy (28,

29). Some of these models are reviewed in (30). In light of the foregoing, we employ an ODE-based approach in the current study. Since we use two types of the DC in immunotherapy, we need a new model incorporating these two types of the DC, which has not been investigated in the previous studies.

Previous studies from our laboratory have demonstrated the increased potential of tumor-specific T-cell induction in the DCs exposed to *Listeria monocytogenes* and the CpG in an experimental tumor immunotherapy model (31-33). Another study revealed that the injection of multiple doses of the DCs matured with *Listeria monocytogenes* result in tumor regression, while multiple doses of the CpG-matured DCs promoted tumor formation (34). Finally, empirical data gathered in that study was used as training data to model the behavior of the immune system against tumor growth. Like other treatment modalities, the main challenge in the DC therapy is when and how much dendritic cells should be administered (35). Therefore, the main contributions of this work include 1) to use of a mathematical model to predict different vaccination patterns for delaying the tumor growth, 2) to evaluate whether the proposed model of combination therapy can increase the antitumor immunity leading to tumor regression. Among different treatment modalities proposed by the model, the combinatorial administration of *Listeria monocytogenes*- and the CpG-matured DCs, showed better results in tumor regression. The organization of the paper is as follows: In Section 2, the experiments are explained, and the proposed model is briefly introduced. The numerical simulations and analysis of the model are summarized in Section 3. Section 4 introduces the work, describes the results, and compares the results with the results of the most similar studies. Section 5 is dedicated to the conclusion, discussion of the findings, and finding a roadmap to ameliorate the suggested model.

MATERIALS AND METHODS

Animals and Cell Lines

Female BALB/c mice (6-8 weeks old) were bought from the Animal Center Lab, Pasteur Institute of Iran. All animal experiments were conducted according to the instructions of the Animal Ethics Committee of Tehran University of Medical Sciences. WEHI164 cell line (fibrosarcoma) which is of BALB/c origin were maintained in RPMI1640 (Biosera, UK), 10% heat-inactivated fetal bovine serum (Gibco, USA), 100 µg/ml streptomycin, 100 U/ml penicillin (Biosera, UK), and 1% L-glutamine (Biosera, UK).

Tumor Lysate (TL) Preparation

6×10^7 tumor cell lines were cultured and resuspended in RPMI1640 medium and then were lysed by 7 rounds of freezing and thawing. The tumor lysed cells were centrifuged at 1500 rpm for 15 min. The protein concentration of the supernatant was measured by bicinchoninic acid (BCA) assay (Thermo Scientific, USA). The supernatant was filtered through a 0.2 µm filter syringe and stored at -20℃ until required.

Oligonucleotides

A synthetic oligodeoxynucleotide (ODN) containing unmethylated Cytosine-b phosphonothioate-guanine (CpG) motifs were purchased from the Alpha DNA Company (Montreal, Canada) including CpG 1826, TCCATG ACG TTC CTG ACG TT; and the control ODN (CPGc), TCC AGG ACT TTC CTC AGG TT.

Generation of Bone Marrow-Derived DC

Generation of bone marrow-derived DCs (BMDCs) was performed according to Inaba protocol with slight modifications (15). In brief, bone marrow cells were flushed from female BALB/c mice femurs and tibia bones and 1×10^6 cells/ml were cultured in RPMI containing 10% FCS, 20 ng/ml Granulocyte-macrophage colony-stimulating factor (GM-CSF) (Peprotech company, USA), and 10 ng/

ml interleukin 4 (IL-4) (Peprotech company, USA). On day 3, non-adherent cells were harvested, and transferred into a new plate, and replaced with a fresh medium. On day 6, 100 µg /ml of tumor lysate (TL) was added, and 4–6 hrs. Later, in some wells 10 µg CpG and other wells 30 mg/ml *Listeria monocytogenses* was added. After 18 hours, the matured DCs were harvested and applied for cancer immune cell therapy.

Tumor Induction and Treatment Protocol

For experimental cancer model establishment, 1.5×10^6 WEHI164 cells (in a total volume of 200 µL) were injected subcutaneously in the right flank of mice. 10^6 DCs matured with CpG and/or *Listeria monocytogenes* were injected around the tumors in distinct groups of mice (n=10 mice per group). The DCs in the List+CpG group were injected according to the pattern predicted by the mathematical model; the Listeria-DCs were injected on day7 after tumor inoculation. The CpG-DCs were injected on day10, and the listeria-DCs were injected on day13 and day16 after tumor inoculation. Table 1 describes all the groups considered in the experimental and computational results of this study. 5 mice in each group were sacrificed on day 23 and the experiment was performed. For assessing the tumor growth, the size of tumors was measured in two dimensions (length x width) every 2 days using digital calipers in the remaining 5 mice.

ELISA for Detection of Secreted Granzyme B

Two weeks after the last immunization, mice spleens were excised and splenocytes were isolated to be used as effector cells. 10^6 splenocytes were co-cultured with WEHI164 cell line as target cells. Cytotoxic activity was measured by the Mouse Granzyme B ELISA kit (eBiosciences, USA). The Granzyme B is present mainly in the granules of $CD8^+$cytotoxic T lymphocytes (CTLs) and natural killer (NK) cells.

Real-time Quantitative PCR

The mice were sacrificed two weeks after the last immunization. For total RNA extraction from the frozen tumor specimens, Trizol-Reagent (Qiagen) was used. For complementary DNA (cDNA) generation, 1 µg of total RNA was reverse transcribed using the QuantiTect Reverse Transcription Kit (Qiagen) following the protocol supplied by the manufacturer. Each DNA sample was amplified in duplicate on an ABI 7500 detection system (Applied Biosystems, USA) using an SYBR Green Real-time PCR master mix (Primer design, UK). Relative quantitation was determined using the comparative Ct method with data normalized to endogenous β-actin as housekeeping gene and calibrated to the average ΔCt of the untreated controls (fold induction = $2^{-\Delta\Delta Ct}$). The sequence of the primers utilized for Real-time PCR amplification is shown in Table 2

Table 1. Different mouse groups and their vaccination pattern.

	Group name	Vaccination time (day)	Material used for maturation	Number of DCs per injection
Calibration data	CpG 1	7	CpG	10^6
	CpG 2	7, 10	CpG	10^6
	CpG 3	7, 10, 13	CpG	10^6
	List 1	7	Lysate of LM*	10^6
	List 2	7, 10	Lysate of LM	10^6
	List 3	7, 10, 13	Lysate of LM	10^6
Validation data	Control	None	None	None
	CpG	7, 10, 13, 16	CpG	10^6
	Listeria	7, 10, 13, 16	Lysate of LM	10^6
	List+CpG	7, 10, 13, 16	CpG: day 10 Lysate of LM: days 7, 13, 16	10^6

* Listeria monocytogenes

Mathematical Model and Simulation

In this study, an ODE-based model is presented to predict the dynamics of antitumor vaccines. The parameters in our model are estimated using empirical data obtained from the previous experiment (34). We call this data *calibration data*. In the next step, we have applied the experimental data of our study (*validation data*) to validate the calibrated model. Table 1 shows the names and specifications of the calibration and validation mouse groups. In the calibration data of (34), 1×10^6 WEHI164 cells were subcutaneously administrated into the right flank of the mouse in a final volume of 200 µl in the cell culture medium. One, two, or three doses of 1×10^6 mature DC (CpG mature DC or Listeria monocytogenes mature DC) were applied around the tumor mass in all the treatment groups of mice on days 7, 10, and 13 after tumor transplantation (one dose only on the 7th day, two doses on the 7th and 10th days and alike). The name the calibration group is as follows: the CpGi represents the group that obtained the "i" dose of the CpG mature DC, and the List thus represents the group that obtained the "i" dose of the Listeria monocytogenes DC. The control group did not obtain any vaccine.

The calibration information includes tumor size, vaccination time, and gene expression of T cell subtypes in laboratory mice. The model presented here consists of six differential equations that translate some of our immunological knowledge into mathematical language. Equations of the model are as follows:

A brief explanation of the model parameters seen in (1)-(6) along with their numerical values can be seen in Tables 1, 3, and 4. The parameters are estimated using minimization of the error between the outputs of the model and the evaluated tumor size in all the mice groups.

Statistical Analysis

Nonparametric means comparisons were performed through a Mann-Whitney test. The comparisons between different groups were performed using one-way ANOVA with Tukey post hoc analysis. The findings are displayed as the means±standard deviation (SD). Kaplan–Meier survival analysis was carried out with the log-rank (Mantel-Cox) test. All calculations were performed on the Graph Pad Prism software (version 5.0). Differences with a P-value<0.05 were considered significant.

RESULTS

Prediction of new patterns

All of the simulations and analyses were conducted in the MATLAB R2017a software.

$$\frac{dT}{dt} = aT(1-bT) - \frac{pET}{g+T} \quad \text{(Tumor cells)} \quad (1)$$

$$\frac{dE}{dt} = -mE - qET + r_1 Th1ET - r_2 TregET + (r_{3L}DC_L + r_{3C}DC_C)\frac{ET}{1+k_1T} + j\frac{TE}{k_2+T} \quad \text{(Effectors cells)} \quad (2)$$

$$\frac{dTh1}{dt} = (\alpha_1 - \beta_1 Th1 - \gamma_1 Treg + \lambda_{1L}DC_L + \lambda_{1C}DC_C)\frac{1}{1+\mu_L DC_L + \mu_C DC_C} \quad \text{(Th1 cells)} \quad (3)$$

$$\frac{dTreg}{dt} = \alpha_2 - \beta_2 Treg - \gamma_2 Th1 + \lambda_{2L}DC_L + \lambda_{2C}DC_C \quad \text{(Treg cells)} \quad (4)$$

$$\frac{dDC_L}{dt} = \sigma_{1L}v_{DCL}(t) + \sigma_{2L}Th1DC_L - \sigma_{3L}TregDC_L - \sigma_{4L}DC_L + \sigma_{5L}\frac{DC_L T}{1+k_{3L}T} \quad \text{(List. matured DCs)} \quad (5)$$

$$\frac{dDC_C}{dt} = \sigma_{1C}v_{DCC}(t) + \sigma_{2C}Th1DC_C - \sigma_{3C}TregDC_C - \sigma_{4C}DC_C + \sigma_{5C}\frac{DC_C T}{1+k_{3C}T} \quad \text{(CpG matured DCs)} \quad (6)$$

Table 2. Primers used in Real time PCR

Sequence	Name
FoxP3	F:5′-TGGCAGAGAGGTATTGAGGG-3′ R:5′- CTCGTCTGAAGGCAGAGTCA-3′
T-bet	F:5′- TCAACCAGCACCAGACAGAC-3′ R:5′- ATCCTGTAATGGCTTGTGGG-3′
Beta-actin	F:5′- TTCTACAATGAGCTGCGTGTG-3′ R:5′- GGGGTGTTGAAGGTCTCAAA-3′

Table 3. Values of immune system dependent parameters used in the model.

Parameters	Description	Estimated value (unit)
a	Tumor growth rate	4.3×10^{-1} (day^{-1})
b	1/b is tumor carrying capacity	2.17×10^{-8} ($cell^{-1}$)
p	Immune system strength coefficient	2×10^{2} (day^{-1})
g	Tumor size necessary for half-maximal effector cell toxicity	1×10^{7} (cell)
m	Death rate of effector cells	2×10^{-2} (day^{-1})
q	Inactivation rate of effector cells by tumor cells	3.4×10^{-10} ($cell^{-1}$ day^{-1})
r_1	Activation rate of effector cells by Th1 cells	7.25×10^{-15} ($cell^{-2}$ day^{-1})
r_2	Inhibition rate of effector cells by Tregs	6.9×10^{-15} ($cell^{-2}$ day^{-1})
j	Activation rate of effector cells by tumor cells	1.245×10^{-2} (day^{-1})
k_1	Inverse of tumor size for CD8+T activation by DCs	5×10^{-7} ($cell^{-1}$)
k_2	Tumor size for half-maximal effector cell activation by tumor cells	2.019×10^{7} (cell)
k_3	Inverse of tumor size for DC activation by tumor cells	2×10^{-8} ($cell^{-1}$)
α_1	Production rate of Th1	4×10^{5} (cell day^{-1})
β_1	Death rate of Th1	9.3×10^{-2} (day^{-1})
γ_1	Inhibition rate of Th1 by Treg	4.2×10^{-2} (day^{-1})
α_2	Production rate of Treg	4×10^{5} (cell day^{-1})
β_2	Death rate of Treg	9.3×10^{-2} (day^{-1})
γ_2	Inhibition rate of Treg by Th1	3.2×10^{-2} (day^{-1})

Table 4. Values of vaccine dependent parameters used in the model.

Parameter	Description	Value (List.)	Value (CpG)	Unit
r_3	Activation rate of CD8+T by DCs	1.95×10^{-12}	1.95×10^{-12}	$cell^{-2}$ day^{-1}
λ_1	Activation rate of Th1 by DCs	2×10^{2}	4×10^{2}	day^{-1}
λ_2	Activation rate of Treg by DCs	2×10^{1}	2×10^{1}	day^{-1}
σ_1	Dendritic cell vaccine coefficient	9.5×10^{4}	9.5×10^{4}	day^{-1}
σ_2	Activation rate of DCs by Th1	1×10^{-8}	1×10^{-8}	$cell^{-1}$ day^{-1}
σ_3	Inhibition rate of DCs by Treg	2×10^{-11}	2×10^{-11}	$cell^{-1}$ day^{-1}
σ_4	Death rate of DCs	1×10^{-1}	1×10^{-1}	day^{-1}
σ_5	Activation rate of DCs by Tumor cells	5×10^{-10}	5×10^{-10}	$cell^{-2}$ day^{-1}
μ	Inverse of DC size for inhibition of Th1	3×10^{-13}	3×10^{-11}	$cell^{-1}$

Figure 1 shows the simulation results with the CpG-matured and *Listeria monocytogenes*-matured vaccines. The vaccination is done on days 7, 10, and 13 (see Table 1 for more details). As can be seen in Figure 1A, injection of one dose of the CpG-matured DC leads to the best results in vaccination with the CpG vaccine. Fast eradication of tumor in the CpG1 is due to the fast increase of Th1 and the lower activation of Treg on the early days, compared to the CpG2 & 3 groups. It should be emphasized that the injection of multiple doses of the CpG vaccine increases the number of Tregs, and provides an immune-

suppressive environment for tumors. This is following the experimental results in our previous study (34).

The opposite happens when the *Listeria monocytogenes* vaccine is given (Figure 1B). That is, with increasing the number of injections, more Th1cells are activated on the early days, making the tumor environment less conducive to its growth. Unlike the CpG vaccine, the increase in Treg is not significant as the number of injections increase, and as a result, the tumor in the List 3 group rapidly suppressed. This is in line with the experimental results in our previous study (36) that indicates *Listeria monocytogenes*-matured DC favors the immune response towards Th1.

It can be seen in Figure 1A that the number of Treg can decrease when inflammatory factors such as Th1 and effector cells increase. After eliminating the tumor, the level of such inflammatory factors reduces, and Tregs can increase to their base level. This process has led to the fluctuations seen in Figure 1 for Tregs.

Next, the model was used to predict a near-optimal vaccination pattern. In this regard, several injection patterns were simulated, and the average tumor size over 30 days was used as a measure of treatment. Only practically applicable patterns were simulated. The results revealed that the best vaccination pattern was related to one-time administration of the CpG matured-DCs on day 10, and 3 administrations of *Listeria monocytogenes*-matured DCs on days 7, 13, and 16 (Figure 2A). The variations of model variables for this combination treatment (List+CpG group) are shown in Figure 2B. As is shown, this vaccination pattern leads to a high rise in Th1 level and a slight stimulation of the Treg, which is an effective treatment for slowing tumor growth. This model prediction was tested experimentally, and the results will be discussed in the following subsections.

Effect of DC Vaccination on Tumor Growth Rate and Survival in Tumor-bearing Animals

We investigated the effect of DC vaccinations on tumor growth rate and survival in different groups. In the List+CpG group, the DCs were injected according to the pattern predicted by the mathematical model (Figure 3A). It is clear from Figs 3B and 3C that multiple doses of matured DCs cause a remarkable reduction of tumor mass size and tumor growth rate. The best result (in the sense of minimum average tumor

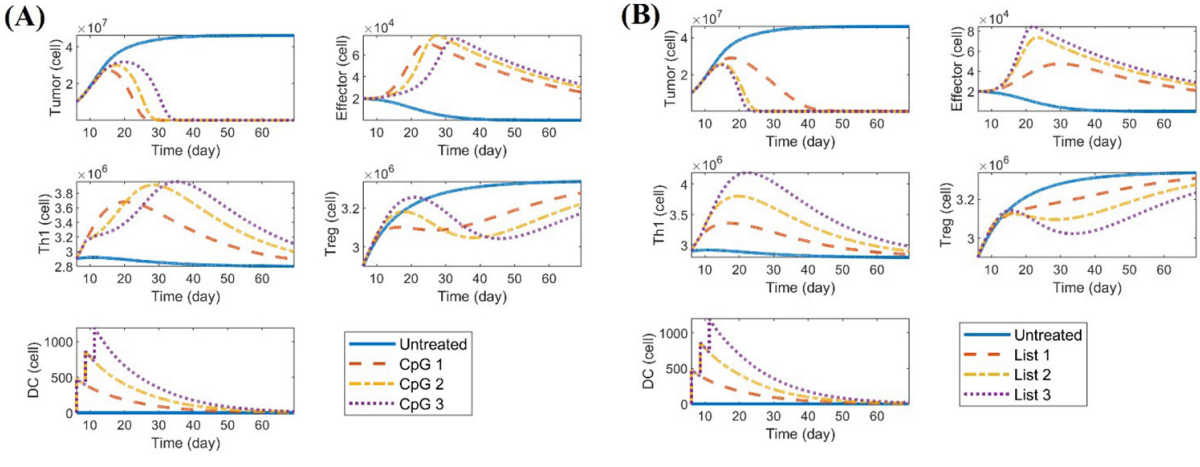

Figure 1. Evaluation of the accuracy of the model according to the data obtained from the previous study. Predictions of the number of Th1, effector cells, Treg, as well as the tumor size during immunotherapy with DC vaccines are shown, loaded with (A) the CpG or (B) *Listeria monocytogenes*. (A) Multiple doses of the CpG-DCs resulted in increased tumor growth, delayed activation of effector and Th1 cells, and increased number of Treg cells. (B) Multiple doses of *Listeria monocytogenes*-DCs resulted in decreased tumor growth, increased activation of effector and Th1 cells, and decreased the number of Treg cells. See Table 1 for more details on vaccination patterns in different groups (Th1=T helper 1, Treg=T regulatory cells, DC=dendritic cell).

size) is achieved in the List+CpG group. As another performance measure, Figure 3D depicts the survival plot for all the groups. It is observed that the *Listeria monocytogenes* group and the List+CpG group had prolonged survival in comparison to the control group.

Effect of DC Vaccination on Foxp3 and T-bet Expression in Tumor-bearing Mice

Th1 cells have a fundamental role in antitumor immune responses and are coordinated by the T-box family of transcription factors (T-bet) genes. In contrast, Treg cells suppress immune responses against tumors promoting the progression of cancer. To determine whether the DC vaccination affects the accumulation of Treg or Th1 cells, the tumors (Figures 4A and C) and spleens (Figures 4B and D) of vaccinated and unvaccinated mice were analyzed for transcript expression of Foxp3 and T-bet as surrogate markers for Treg and Th1

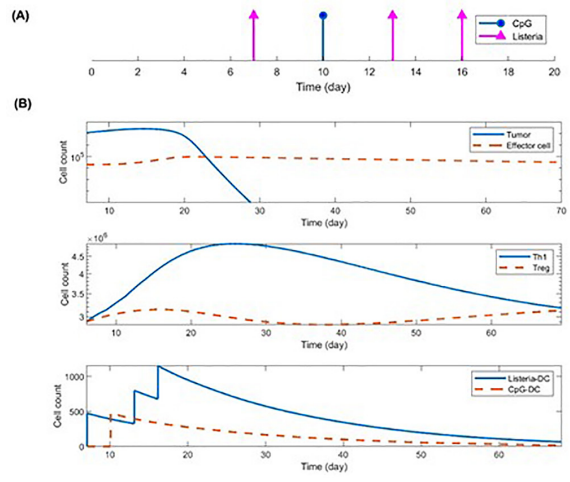

Figure 2. The mathematical model simulations for the List+DC group. (A) The pattern of the DC vaccine administration was selected from among several patterns predicted by the mathematical model (data not shown). (B) The simulated number of tumor cells, effector cells, Th1, Treg, and DCs during vaccination. With this pattern of the DC vaccination, tumor growth decreased, Th1 numbers reached the maximum level, and Treg cells reduced to their minimum level compared to other predicted patterns (data not shown).

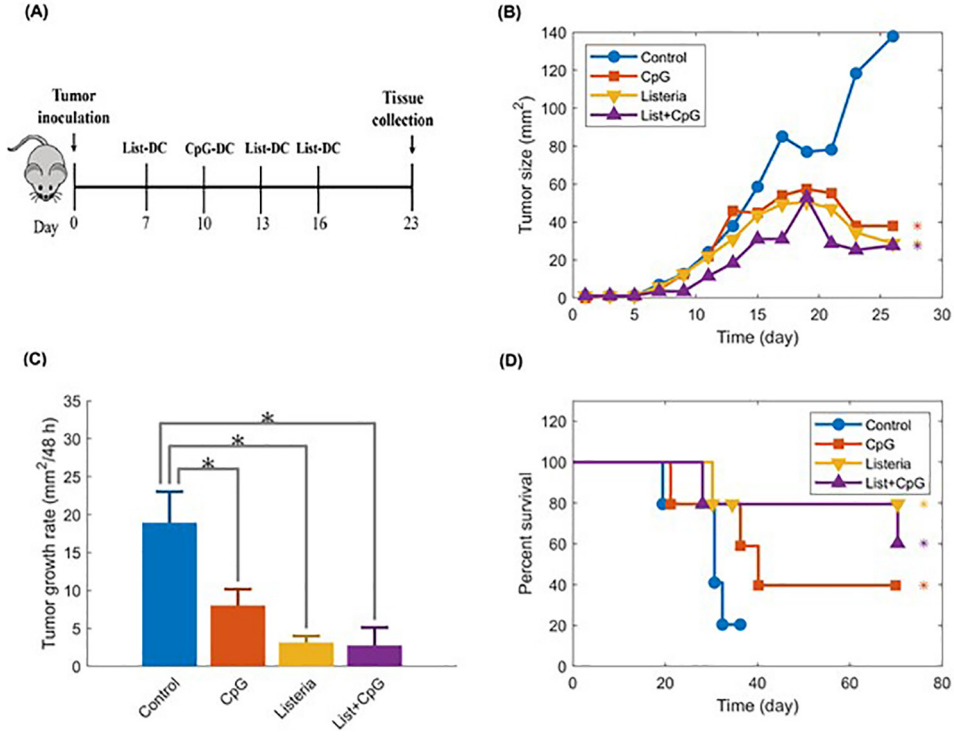

Figure 3. Effect of DC vaccination on tumor growth rate and survival in tumor-bearing mice. BALB/c mice were injected subcutaneously with 1.5×10^6 WEHI 164 fibrosarcoma cells. See Table 1 for more details on vaccination patterns in different groups. (A) Schematic diagram of the experiments, (B) Tumor size reported in mm^2 was followed for up to 30 days, (C) the mean tumor growth per 48 hrs. in different groups (n=5, *P<0.05 by one-way ANOVA). (D) Survival of the animals in each group was monitored and the respective Kaplan–Meier curves are given (n=5; *P<0.05).

respectively using RT-PCR. The data showed a significant decrease in Foxp3 and a meaningful increase in the expression state of the T-bet factor in the spleen of all the treatment groups. Furthermore, analysis of the tumor tissues revealed an increased expression of Foxp3 in mice receiving the CpG-DC compared to the other groups. However, the expression of T-bet in tumor tissues significantly elevated in animals treated with *Listeria monocytogenes*-matured DCs.

Effect of DC Vaccination on Cytotoxic Activity of Lymphocytes in Tumor-bearing Mice

The effects of various treatment modalities on the cytolytic capacity of spleen cells were assessed by measuring the granzyme B secretion. The splenocytes were isolated from mice, then incubated with WEHI164 tumor cells for six hours and the secretion of granzyme B was evaluated. As illustrated in Figure 5, a considerable increase of granzyme B secretion in the *Listeria monocytogenes* group and a slight increase in the List+CpG group were observed compared to the untreated group. As we expected, numerous doses of the CpG-matured DCs did not induce any considerable cytotoxic activity.

Comparison of Experimental and Simulation Results

Figure 6 compares tumor growth predictions and experimental results in all the groups. Since the tumor size in the experimental data is measured in mm^2, and its unit in the model is the number of cells, for comparability of units, we converted mm^2 to the number of cells by the following transformation:

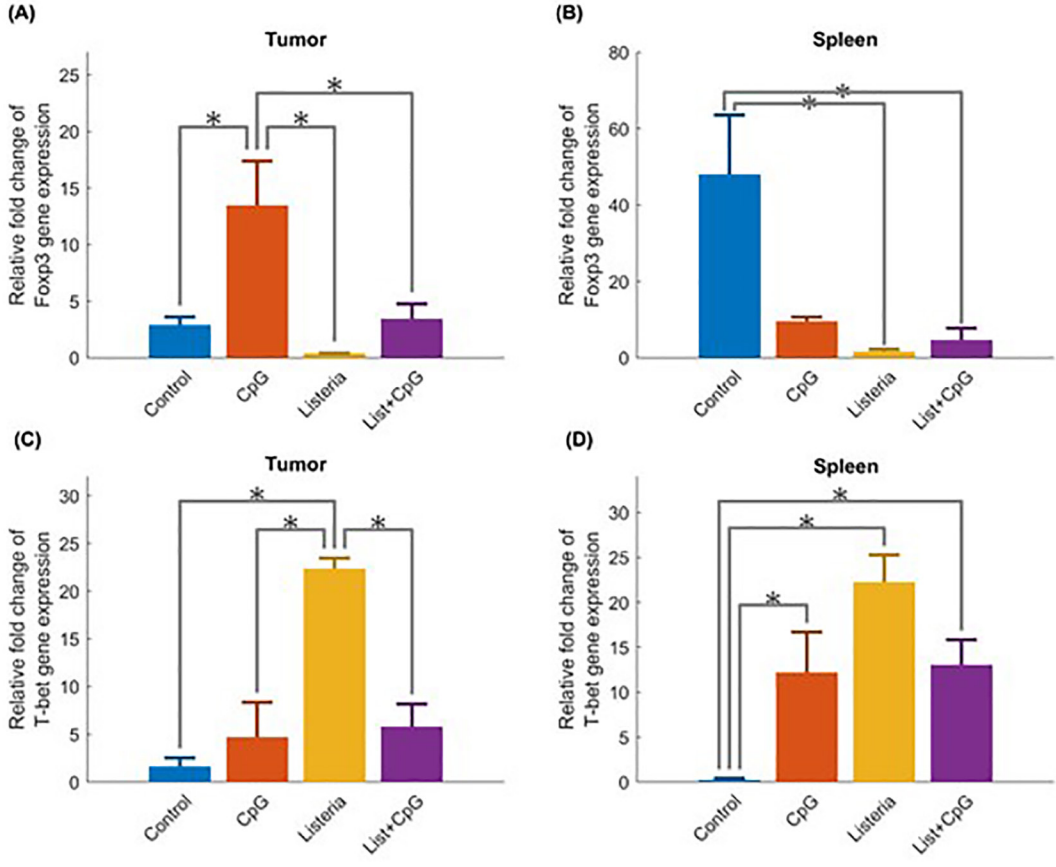

Figure 4. Expression of (A-B) FoxP3 and (C-D) T-bet mRNA in tumor and spleen. See Table 1 for more details on vaccination patterns in different groups. Mice were sacrificed one week after the last vaccination in all the groups, and the tumor and spleen tissues were separated. Total RNA was extracted, and the expression of FoxP3 and T-bet was assessed by quantitative reverse transcription real-time PCR in tumor (left) and spleen (right) tissues. Bars indicate the mean±SEMs; *P < 0.05, n=5. Average values from three different experiments are shown.

$$Tumor_{cell} = 2.53 \times 10^5 \times Tumor_{mm^2} + 10^7 (7)$$

As shown in Figure 6A, the List+CpG group has the best result in tumor size decrease, but there is no meaningful difference between this group and *Listeria monocytogenes* group. In simulation results, the List+CpG group could reduce tumor size more than the other groups because of more Th1 activation in the early days of injections and less activation of Treg.

Comparing the experimental and the simulation results in all the four groups (Figure 6 C-F) shows that these two results are in relatively good agreement. As an instance, in the CpG group, the model has predicted a stable tumor size in the final days, which is confirmed by the experimental results. It should be noted that since the experimental results are stochastic in nature, the results are highly dependent on sample size, and thus, it

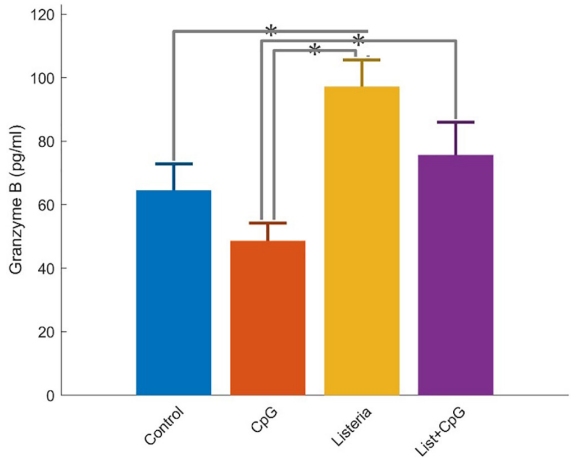

Figure 5. Tumor-specific cytotoxic responses induced by the DC vaccines in tumor-bearing mice. See Table 1 for more details on the vaccination patterns in different groups. Effector cells (Splenocytes) were obtained from mice and co-cultured with target cells (WEHI 164) and then the concentration of Granzyme B was measured in culture supernatants (ELISA). Bars indicate the mean±SEM. Average values from three different experiments have been shown (*P<0.05; n=3)

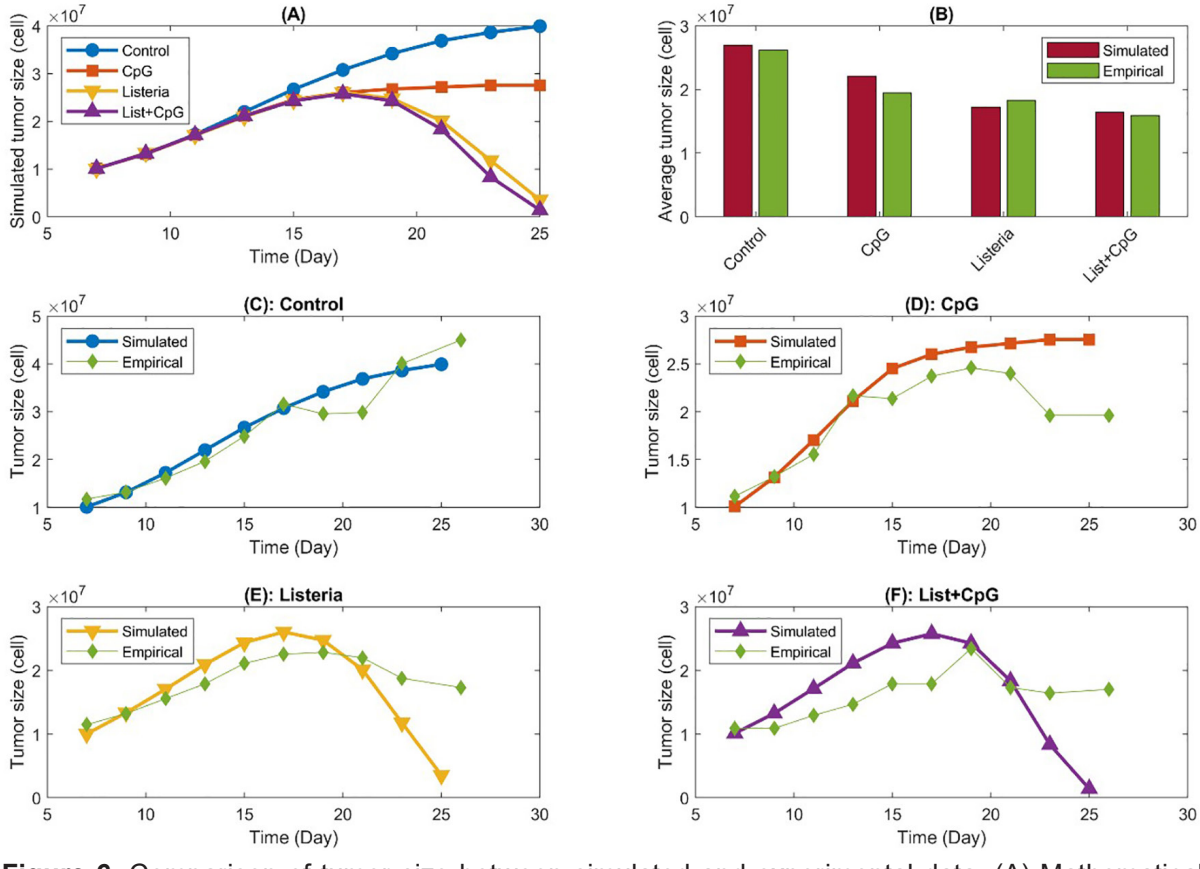

Figure 6. Comparison of tumor size between simulated and experimental data. (A) Mathematical simulation of tumor size in four groups with different treatments, (B) Comparison of average tumor size between simulated and empirical data in each group separately, (C-F) Comparison of tumor size between the experimental results and simulations for each group separately. See Table 1 for more details on vaccination patterns in different groups.

is normal to see some differences between the measured and the simulated results. This is well seen in the List+CpG group, where there is a relatively large error in model predictions for tumor size in the last few days. But, if we consider the average of tumor size over all-time points, we witness the model has made a relatively accurate prediction for tumor size in all the groups. Figure 6 B compares the average of tumor size over all-time points for all the groups, both in simulated and empirical data.

For further investigation, Figure 7A shows the comparison between the experimental and predicted data for FoxP3 expression level. As seen in this figure, both the simulation and the experimental results show a high value for Foxp3 expression in the CpG group. For other groups, the expression level of Foxp3 does not differ significantly in both the simulation and the empirical results.

Figure 7B depicts the predicted and measured values for T-bet gene expression in different groups. Both the simulation and the experimental results show relatively similar results for T-bet expression in the control, the CpG, and *Listeria monocytogenes* groups. However, the results in the List+CpG group are different.

DISCUSSION

Despite impressive advances in understanding the molecular and cellular basis of cancer, it remains one of the major causes of morbidity and mortality on a global scale, (37) and poor or late diagnosis of cancer makes it difficult to be treated (38). Over the years, there have been numerous cancer treatment approaches discovered. Especially, DC-based immunotherapy has become the focus of extensive scientific and clinical researches.

DC vaccine trials meet some challenges

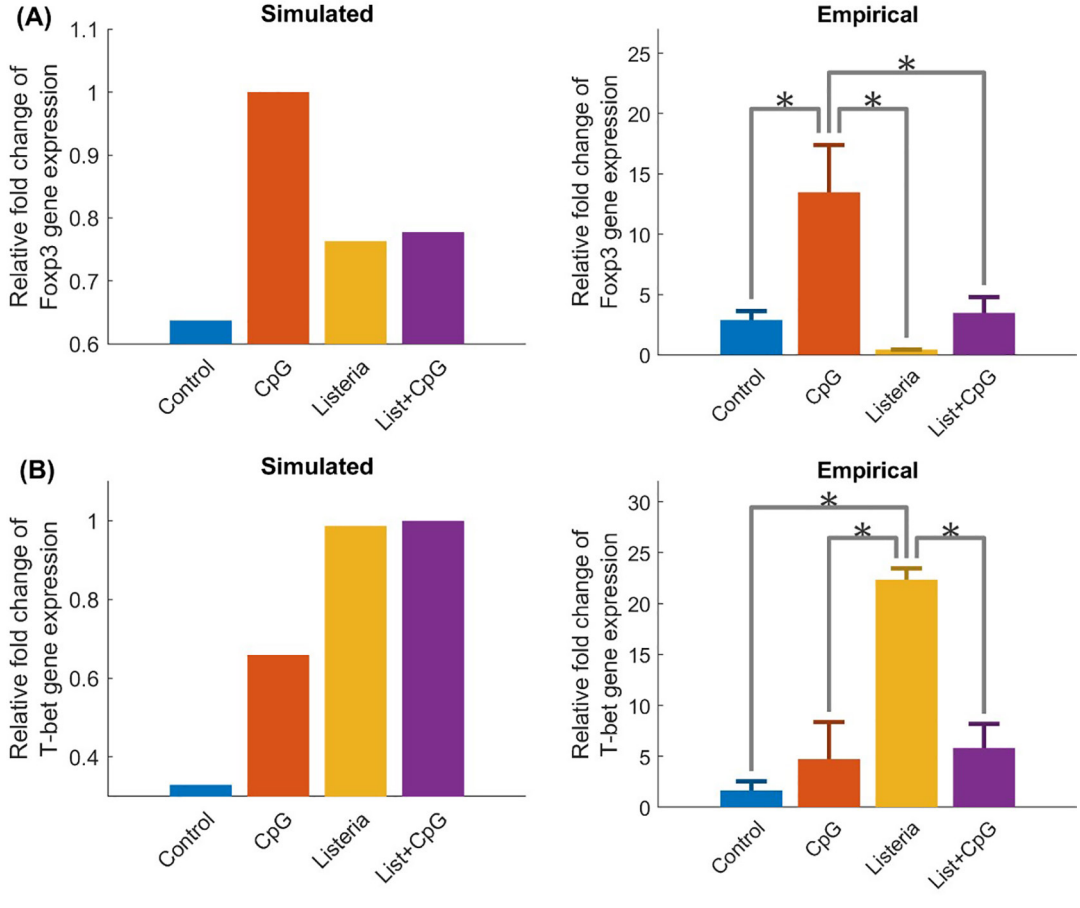

Figure 7. Comparison of (A) Foxp3 and (B) T-bet expression levels between simulated and experimental data. See Table 1 for more details on vaccination patterns in different groups

including the time of DC vaccine injections, failure to elicit both $CD4^+$ / $CD8^+$ T cell response, high costs, and time-consuming processes (39-41). These challenges can be mitigated by mathematical models of cancer immunotherapy that can then be used to predict an optimal treatment protocol. Knowledge about tumor-immune interactions and clinical studies about cancer immunotherapy has been enhanced through the use of mathematical and in silico models (42). Mathematical modeling and simulation are especially useful in immunology. These models have been developed to evaluate numerous possible dose administration strategies and combination schedules to select the pattern which increases patient survival.

Different mathematical models have been employed to describe the dynamics of the immune system and the tumor, including the most popular of them, namely, ODE. ODE helps to understand the dynamics of a particular system, as well as find proper treatment options, predict the optimal dose and the right time of vaccine administration and propose the best option for efficient treatments (43, 44). De Pillis et al. designed a mathematical model based on the ODEs to evaluate cancer growth treated by a combination of immunotherapy and chemotherapy (43). Fouchet and Regoes used a mathematical model to describe an interaction network of adaptive regulatory T cells, depending on the activation state of antigen-presenting cells (45). Mathematical modeling also has been applied for DC vaccine approaches. Pappalardo et al. developed an ordinary differential equation model to evaluate how many and how frequent booster of DC vaccines is needed to sustain a long-lasting and protecting memory T cell response against tumor antigens (46).

Mathematical modeling and simulation are especially applicable in immunology as it permits to predict and design un-experimented clinical trials as well as dose selection. Mathematical modeling of the immune system is very complicated because of a complex interaction between immune cells and the tumor microenvironment; therefore, models that simulate the immune responses against the tumor should only focus on certain components of the immune system depending on the model (15, 47, 48). Mathematical models based on the ODE are the most common models used in cancer immunotherapy (49, 50).

A former study indicated that the administration of a single dose of the DCs matured with *Listeria monocytogenes* and the CpG induced a detectable Cytotoxic T cell-dependent antitumor immunity and also tumor regression (31, 32). In the present study, we have conducted another experiment to assess the effect of multiple doses of the DCs matured with these two maturation factors against tumors. Our results show that multiple injections of *Listeria monocytogenes* matured-DCs induced effective antitumoral immune response and notably reduced the tumor formation measure. On the contrary, numerous doses of the CpG-exposed DCs, unlike one-time administration, did not augment the antitumor immune response.

In the present study, and to find near-optimal scheduling of the DC vaccine interventions, we used empirical data from previous studies including tumor growth rate and days of the DCs administration to model the dynamics of antitumor vaccines and predict the pattern of vaccine administration. In other words, we stimulate the interaction between tumor and immune system based on data from previous studies, using ODEs. Therefore, our model could predict the outcome of immunotherapy with combined vaccines. The mathematical model suggested that the combination of both vaccines of the CpG and *Listeria monocytogenes*, on certain days, had more favorable results in the activation of the immune system. Appropriate treatment protocol which yielded better results in the simulations, was related to the combination of *Listeria monocytogenes* and the CpG vaccine administration on days 3, 7, 10, and 13 after the tumor inoculation.

It should be noted that we cannot claim that the proposed treatment protocol is an optimal one because we have tested a limited number of practical patterns of vaccinations by changing the dose and the time of injection in a trial-and-error manner, and we have not used an optimization algorithm that guarantees the optimality of the final answer. Therefore, the optimality of the obtained model was tested only among the applicable answers.

Various studies have indicated that the best evaluation criteria for mathematical model accuracy of the DC therapy would be its impact on reducing the tumor size (51-53). Our results indicated that the tumor growth rate in the List+CpG and *Listeria monocytogenes* groups reduced similarly and significantly in comparison with the control group. However, the reduction of tumor size means in the List+CpG group was slightly greater than in the *Listeria monocytogenes* group. Therefore, in this study, the combination therapy group was effective in reducing the tumor size. Several studies have indicated that the Foxp3 expression is associated with invasion, angiogenesis, size, and immune-suppression of tumors. Thus, these studies suggest a utility of Foxp3 as a marker of tumor progression and metastasis and an indicator of Treg activity (37-39). Our results demonstrated that the expression of Foxp3 in a List+CpG group was almost similar to the results predicted by mathematical models.

A previous study has demonstrated that a single dose of CpG-mature DC led to tumor regression (18). This study showed that numerous doses of CpG mature DC significantly increased the tumor growth and reduced the survival rate. As a result, we hypothesized that we can take advantage of the single CpG-matured DC vaccination to have a significant antitumor immune response in our mathematical model. In the present study, our results are related to the CpG group align with previous studies indicating that multiple doses of the CpG administration exacerbate tumor growth.

The closest study to this work is (18) in which an ANN model predicts a decreasing injection pattern for the CpG matured DCs (10^6, 5×10^5 and 10^5 cells on days 7, 11, and 15, respectively), as well as an increasing injection pattern for *Listeria monocytogenes*-matured DCs (10^5, 5×10^5, and 10^6 cells on days 7, 11, and 15, respectively) as the optimal injection pattern (we call it the decreasing-increasing pattern). Figure 8 compares the simulation and experimental results of this injection pattern with the results of the List + CpG group in our study. Simulations of both patterns were performed by the model presented in this study. As is clear in Figure 8A, our model predicts that the List+CpG pattern will reduce tumor size more effectively than the decreasing-increasing pattern. Comparison of experimental tumor size in these two groups in Figure 8B confirms this perdition. It should be noted that these two data sets have been gathered in different times and conditions, and we need to be more cautious in comparing them. We have concluded that the differences between the results predicted by the mathematic model and experimental results arose from the equations of the model and should be modified. In general, assessing Treg and Th1 expression is not enough for predicting tumor behavior and, probably other intermediate variables, for example, Th17 cells in interaction with other cells can provide us with a better understanding. Therefore, it can be concluded that phases related to effector cells (variable E (t): effectors cells number in the model) should be modified. In addition, we need to have more data to do a more accurate simulation. As an instance, it is necessary to kill the mice, from the first day of the DC vaccination administration and in vivo testing, in addition to gene expression analysis to be performed. But it is not possible in the laboratory due to time constraints and also material and equipment costs. Therefore, it is better to use older and classic models like agent-based models instead of the ODE models, which require less data for training. Although previous study data has been

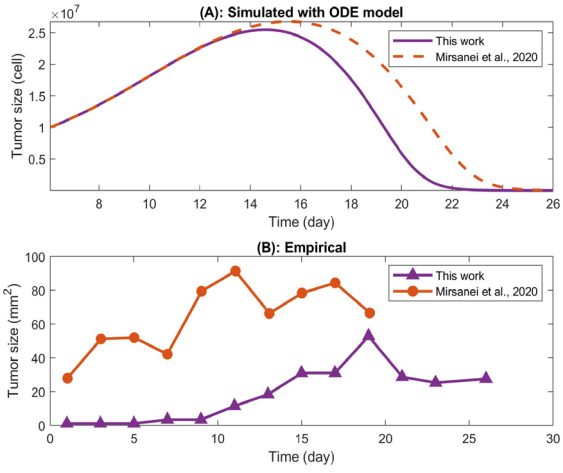

Figure 8. Comparison of the results of this work and those of (Mirsanei et al. 2020). (A) Predicted tumor size when the vaccination patterns is based on the List+CpG group of this work (solid) or is according to the predicted patterns of (Mirsanei et al. 2020) (dashed). Both patterns were simulated using the ODE model of this work. (B) Empirical tumor size in the List+CpG group of this work (▲) compared to measured tumor size reported in (Mirsanei et al., 2020) (●).

used for our model, the model was able to predict the behavior of the system regarding the tumor size according to simulation and experimental results. This demonstrates the validity of the mathematical model. However, in an earlier study (30), the administration of the CpG-matured DC vaccine began on day 7 after the tumor inoculation while in our study, the injections started on day 10 which can be the reason for the observed differences in the results of the previous and the current studies.

CONCLUSION

Taken together, a mathematical model based on differential equations was able to approximately predict the results of the DC vaccination in the List+CpG group, and the prediction regarding the tumor size was more accurate. Results of immunotherapy in different groups indicated in the combined therapy group were more effective in the decline of tumor size in comparison with the other groups. However, the T-bet expression in the treatment group with the DC vaccine matured with *Listeria monocytogenes* was higher than in the other groups. In the case of Foxp3 gene expression, combined treatment, and *Listeria monocytogenes* groups, the results are almost the same. As expected concerning the CpG-matured DC group (47), by increasing the number of injections, Foxp3 expression increased while there was no meaningful intensity in the expression of the T-bet gene. Hence, by setting some parameters, coefficients, and equations including the equation of effector cells, we can improve the results of the combined vaccines. This study has several limitations and potential future directions as coming below:

- The differences between the experimental data and the model results are large in some cases. This may be due to the measurement error, the low number of experimental samples, or weak model prediction. By performing experiments with more samples, the immunological rules used in the model can be reconsidered.
- Some of the estimation parameters of the model differ significantly from the values reported in other similar studies. Several estimated parameters (e.g. related to Th subgroup generation and turnover) can be evaluated experimentally. In other previous studies, these items were assessed for the whole circulating lymphocytes, but not for each Th subgroup separately. Experimental estimation of these parameters improves the accuracy of the model.
- For suppleness, the roles of Th2 and Th17 cells are not incorporated into the suggested model, but the experimental information is accessible for these cells. In future studies, the above-mentioned cells may be included individually in the model using new trial data.
- Consideration of the immune evasion of the tumor, which can be mediated by different agents (like adenosine

and HIF-α), adding more precise characterizations of the underlying mechanisms to the model of the tumor-immune interactions. It needs more experimental data and more combinations of vaccines.

- Highlighting more effective parameters in this model through a sensitivity analysis can make the model simpler by removing the less important expressions. This approach achieves a simpler model, capable of being applied for theoretical and numerical analyses, such as equilibrium point analysis, bifurcation analysis, etc., to give a better view of the dynamics in the system, and highlight the potential targets in the treatment.

ACKNOWLEDGMENT

This study was supported by grant number 25721 from Tehran University of Medical Sciences and Cancer Biology Research Center, Cancer Institute of Iran, Tehran University of Medical Sciences.

Conflict of Interest: None declared.

REFERENCES

1. Rebecca L. Siegel M, M. Kimberly D. Miller, and D. Ahmedin Jemal. Cancer Statistics. CA CANCER J CLIN. 2015;65: p. 5-29
2. Parkin DM, Bray F, Ferlay J, Pisani P. Global cancer statistics, 2002. CA Cancer J Clin. 2005;55(2):74-108.
3. Siegel RL, Miller KD, Jemal A. Cancer statistics, 2016. CA: a cancer journal for clinicians. 2016;66(1):7-30.
4. Gotwals P, Cameron S, Cipolletta D, Cremasco V, Crystal A, Hewes B, et al. Prospects for combining targeted and conventional cancer therapy with immunotherapy. Nature Reviews Cancer. 2017;17(5):286-301.
5. Arina A, Gutiontov SI, Weichselbaum RR. Radiotherapy and immunotherapy for cancer: From "systemic" to "multisite". Clinical Cancer Research. 2020;26(12):2777-82.
6. Sharma P, et al. Novel cancer immunotherapy agents with survival benefit recent successes and next steps. Nature Reviews Cancer. 2011;11(11):p. 805-12.
7. Khosravianfar N, Hadjati J, Namdar A, Boghozian R, Hafezi M, Ashourpour M, et al. Myeloid-derived Suppressor Cells Elimination by 5-Fluorouracil Increased Dendritic Cell-based Vaccine Function and Improved Immunity in Tumor Mice. Iran J Allergy Asthma Immunol. 2018;17(1):47-55.
8. Arab S, Motamedi M, Hadjati J. Effects of dendritic cell vaccine activated with components of Leishmania major on tumor specific response. Iranian Journal of Immunology. 2019;16(4):268-77.
9. Zanna MY, Yasmin AR, Omar AR, Arshad SS, Mariatulqabtiah AR, Nur-Fazila SH, et al. Review of dendritic cells, their role in clinical immunology, and distribution in various animal species. International Journal of Molecular Sciences. 2021;22(15):8044.
10. Behboudi S CD, Klenerman P Austyn J. The effects of DNA containing CpG motif on dendritic cells. Immunology. Immunology. 2000 March;99(3):361–6.
11. Hirata N, Yanagawa Y, Satoh M, Ogura H, Ebihara T, Noguchi M, et al. Dendritic cell-derived TNF-alpha is responsible for development of IL-10-producing CD4+ T cells. Cell Immunol. 2010;261(1):37-41.
12. Wischke C, Zimmermann J, Wessinger B, Schendler A, Borchert HH, Peters JH, et al. Poly(I:C) coated PLGA microparticles induce dendritic cell maturation. Int J Pharm. 2009;365(1-2):61-8.
13. Arab S, Mojarrad M, Motamedi M, Mirzaei R, Modarressi M, Hadjati J. Tumour Regression Induced by Co-administration of MIP-3α and C p G in an Experimental Model of Colon Carcinoma. Scandinavian journal of immunology. 2013;78(1):28-34.
14. Safvati A, Allahverdy A, Zandi S, Rahbar S, Mirzaei HR, Mirsanei Z, et al. A predictive approach for the tumor-immune system interactions based on an agent based modeling. Frontiers in Biomedical Technologies. 2015;2(4):214-26.
15. Castiglione F, Piccoli B. Cancer immunotherapy, mathematical modeling and optimal control. Journal of Theoretical Biology. 2007;247(4):723-32.
16. Duun-Henriksen AK, Schmidt S, Røge RM, Møller JB, Nørgaard K, Jørgensen JB, et al. Model identification using stochastic differential equation grey-box models in diabetes. Journal of diabetes science and technology. 2013;7(2):431-40.
17. Mehrian M, Asemani D, Arabameri A,

Pourgholaminejad A, Hadjati J. Modeling of tumor growth in dendritic cell-based immunotherapy using artificial neural networks. Computational biology and chemistry. 2014;48:21-8.
18. Mirsanei Z, Habibi S, Kheshtchin N, Mirzaei R, Arab S, Zand B, et al. Optimized Dose of Dendritic Cell-based Vaccination in Experimental Model of Tumor Using Artificial Neural Network. Iranian Journal of Allergy, Asthma and Immunology. 2020:172-82.
19. Arabameri A, Pourgholaminejad A. Modeling codelivery of CD73 inhibitor and dendritic cell-based vaccines in cancer immunotherapy. Computational Biology and Chemistry. 2021:107585.
20. Yang HM. Mathematical modeling of solid cancer growth with angiogenesis. Theoretical Biology and Medical Modelling. 2012;9(1):1-39.
21. Rhodes A, Hillen T. A mathematical model for the immune-mediated theory of metastasis. Journal of theoretical biology. 2019;482:109999.
22. Mahasa KJ, Ouifki R, Eladdadi A, de Pillis L. Mathematical model of tumor–immune surveillance. Journal of theoretical biology. 2016;404:312-30.
23. Kuznetsov VA, Knott GD. Modeling tumor regrowth and immunotherapy. Mathematical and Computer Modelling. 2001;33(12-13):1275-87.
24. Das P, Mukherjee S, Das P, Banerjee S. Characterizing chaos and multifractality in noise-assisted tumor-immune interplay. Nonlinear Dynamics. 2020;101(1):675-85.
25. Das P, Das S, Das P, Rihan FA, Uzuntarla M, Ghosh D. Optimal control strategy for cancer remission using combinatorial therapy: a mathematical model-based approach. Chaos, Solitons & Fractals. 2021;145:110789.
26. de Pillis LG, Gu W, Radunskaya AE. Mixed immunotherapy and chemotherapy of tumors: modeling, applications and biological interpretations. Journal of theoretical biology. 2006;238(4):841-62.
27. Kirschner D, Panetta JC. Modeling immunotherapy of the tumor–immune interaction. Journal of mathematical biology. 1998;37(3):235-52.
28. Huang W-z, Hu W-h, Wang Y, Chen J, Hu Z-q, Zhou J, et al. A mathematical modelling of initiation of dendritic cells-induced T cell immune response. International journal of biological sciences. 2019;15(7):1396.
29. Dickman LR, Milliken E, Kuang Y. Tumor control, elimination, and escape through a compartmental model of dendritic cell therapy for melanoma. SIAM Journal on Applied Mathematics. 2020;80(2):906-28.
30. Arabameri A, Asemani D, Hadjati J. A structural methodology for modeling immune-tumor interactions including pro-and anti-tumor factors for clinical applications. Mathematical biosciences. 2018;304:48-61.
31. ARAB S, Motamedi M, KHANSARI NE, GHEFLATI Z, HAJATI J, MOAZENI S. Dendritic cell maturation with CpG for tumor immunotherapy. 2006.
32. Khamisabadi M, Arab S, Motamedi M, Khansari N, Moazzeni SM, Gheflati Z, et al. Listeria monocytogenes activated dendritic cell based vaccine for prevention of experimental tumor in mice. Iranian Journal of Immunology. 2008;5(1):36-44.
33. Mirzaei R, Arab S, Motamedi M, Amari A, Hadjati J. The Opposite Effects of DNA and Protein Components of Listeria Monocytogenes and Toxoplasma gondii on Immunologic Characteristics of Dendritic Cells. Iran J Allergy Asthma Immunol. 2015;14(3):313-20.
34. Pourgholaminejad A, Jamali A, Samadi-Foroushani M, Amari A, Mirzaei R, Ansaripour B, et al. Reduced efficacy of multiple doses of CpG-matured dendritic cell tumor vaccine in an experimental model. Cellular immunology. 2011;271(2):360-4.
35. Peng H1 ZW, Tan H1, Ji Z1, Li J2, Li K1, Zhou X1. Prediction of treatment efficacy for prostate cancer using a mathematical model. Sci Rep. 2016; 12(6):21599.
36. MOTAMEDI M, Arab S, KHANSARI NE, Moazeni S, VOJGANI M, KEYHANI A, et al. Effect of Listeria monocytogenes on tumor immunotherapy with dendritic cells. 2007.
37. Ma X, Yu H. Global burden of cancer. Yale J Biol Med. 2006;79(3-4):85-94.
38. Cancer Care for the Whole Patient: Meeting Psychosocial Health Needs. Washington (DC): National Academies Press (US); 2008.
39. Schaller TH, Sampson JH. Advances and challenges: dendritic cell vaccination strategies for glioblastoma. Expert Review of Vaccines. 2017;16(1):27-36.
40. Chen P, Liu X, Sun Y, Zhou P, Wang Y, Zhang Y. Dendritic cell targeted vaccines: Recent progresses and challenges. Hum Vaccin Immunother. 2016;12(3):612-22.
41. Mantia-Smaldone GM, Chu CS. A review of dendritic cell therapy for cancer: progress and challenges. BioDrugs. 2013;27(5):453-68.
42. Byrne HM. Dissecting cancer through mathematics: from the cell to the animal model. Nat Rev Cancer. 2010;10(3):221-30.
43. de Pillis LG, Gu W, Radunskaya AE. Mixed immunotherapy and chemotherapy of tumors: modeling, applications and biological interpretations. J Theor Biol. 2006;238(4):841-62.
44. Eftimie R, Bramson JL, Earn DJ. Interactions

between the immune system and cancer: a brief review of non-spatial mathematical models. Bull Math Biol. 2011;73(1):2-32.
45. Fouchet D, Regoes R. A population dynamics analysis of the interaction between adaptive regulatory T cells and antigen presenting cells. PLoS One. 2008;3(5):e2306.
46. Pappalardo F, Pennisi M, Ricupito A, Topputo F, Bellone M. Induction of T-cell memory by a dendritic cell vaccine: a computational model. Bioinformatics. 2014;30(13):1884-91.
47. Andrew SM, Baker CTH, Bocharov GA. Rival approaches to mathematical modelling in immunology. Journal of Computational and Applied Mathematics. 2007;205(2):669-86.
48. Eftimie R, Gillard JJ, Cantrell DA. Mathematical Models for Immunology: Current State of the Art and Future Research Directions. Bull Math Biol. 2016;78(10):2091-134.
49. Brodland GW. How computational models can help unlock biological systems. Seminars in Cell & Developmental Biology. 2015;47:62-73.
50. Sbeity H YR-dj. Review of Optimization Methods for Cancer Chemotherapy Treatment Planning. J Comput Sci Syst Biol. 2015;8(1):74-95.
51. Hartung N, Mollard S, Barbolosi D, Benabdallah A, Chapuisat G, Henry G, et al. Mathematical modeling of tumor growth and metastatic spreading: validation in tumor-bearing mice. Cancer Res. 2014;74(22):6397-407.
52. Osipov OGIaVA. Different Strategies for Cancer Treatment: Mathematical Modelling. Computational and Mathematical Methods in Medicine. 2009;10(4):Pages 253-72.
53. Uhr KPJ. Mathematical models of cancer dormancy. Leukemia & Lymphoma. 2005;46(3):313-27.